Recent development in instrumentation of automated grating interferometry

M. Kujawińska, L. Sałbut

Institute of Design of Precise and Optical Instruments, Warsaw University of Technology, ul. Chodkiewicza 8, 02–525 Warszawa, Poland.

High sensitivity grating interferometry has been proved to be the effective experimental tool in mechanics and material science. However, recent measurement requirements connected with new applications form several challenging instrumentational and software requests, including analysis of transient events, macro- and microscale measurement ability, measurements directly on a standard loading machine, full automatization of acquisition of data and analysis of the results, interaction with FEM, BEM and other application oriented software. The paper presents the series of automated grating interferometers, including the laboratory, workshop and sensor-type systems which can alternatively fulfil the modern measurement requirements. The systems enable the adaptive fringe pattern design and automated analysis based on temporal, spatial and spatial-carrier phase shifting techniques. The usefulness of automated grating interferometry systems is shown through wide selection of recent applications, including fracture mechanics, residual stresses determination, relaxation processes, fatigue testing, local material constant measurements and many others.

1. Introduction

Recently, grating (moiré) interferometry is one of the most popular optical methods used in experimental mechanics and material science [1]. It has excellent characteristics, such as: real-time, whole-field mapping, submicrometer sensitivity, high interference fringes contrast, wide strain range and easy alignment and operation. However, the modern applications of grating interferometry as an experimental tool in hybrid methods of stress analysis [2], [3] widen the list of requirements which should be fulfilled by this method. The most challenging problems are connected with micromechanics and new technological material testing, including fracture mechanics, relaxation processes, fatigue testing, heat-transfer problems, residual stresses, contact problems, determination of local material constants and many others. The experimental technique dealing with such problems should enable:

— determination of in-plane u and v and out-of-plane w displacement maps in whole field with high resolution (*e.g.*, 512×512 sampling points),

— analysis of dynamic event, which means simultaneous capturing of data about u, v and w displacement fields,

— continuous monitoring of u, v, w displacement fields,

— measurements in unstable environment, *e.g.*, directly on a standard loading machine,

— possibility to design a specialized, compact fibre optics sensor which enables measurements directly on the mechanical structure,

— adaptivity of the system for macro- and microscale measurements,

— adaptivity of the system to work at elevated temperatures and over long period of time,

— adaptivity of optomechanical arrangement for the proper fringe pattern design system to match to the best fitted automated interferogram analysis in the application considered,

— automatic analysis of the experimental result with the output in the form of displacement and/or strain maps and local material constants distribution (*e.g.*, Poisson ratio, Young's moduli),

— compatibility of the results with the requirements for the input data for numerical methods of stress analysis (FEM, BEM).

The aim of the paper is to present optomechanical grating interferometry systems coupled with automated interferogram analysis which have capability to become the experimental tool in hybrid tchniques for analysis and modelling modern problems in experimental mechanics and material engineering.

Due to great variation of the requirements, they cannot be simultaneously fulfilled by a single system. That is the reason why three basic types of automated grating interferometers (AGI) were proposed and designed: the laboratory (LGI) [4]−[7], workshop (WGI) [8], [9], and sensor type (FOS) [10] systems.

The laboratory system is understood as open optomechanical arrangement easy to modify for various experimental requirements, providing high accuracy results, however, demanding stable conditions (stabilized tables, constant temperature, *etc.*) and operated by a specialist. The laboratory system can be easily modified to provide additional information about out-of-plane displacement.

The workshop portable system is a compact system which is much less sensitive to vibrations, easy to operate, however, the accuracy of the measurement may be lower and it cannot be easily modified. It is used for the analysis of influence of environmental changes (in temperature chamber), analysis of transient events and the measurement directly on a standard loading machine.

The sensor-type system is a specialized fibre optic realization of grating interferometer. Its small size, compactness and resistance to vibrations enable us to use the sensor directly at machine and civil engineering structures. This last system is indicated here more like a future recommendation than the actually operating sensor, although the preliminary works on its modelling and design have been done [10].

Although the optomechanical arrangements in all three cases are different, the methodology of displacement measurement and analysis of the results is similar. It is presented in Fig. 1.

As the system has to enable the analysis of interferogram captured under various conditions, including transient events and measurement in unstable environment, the special attention should be paid to the problem of fringe pattern design and its capturing in one- or multichannel optomechanical arrangements. The analysis of
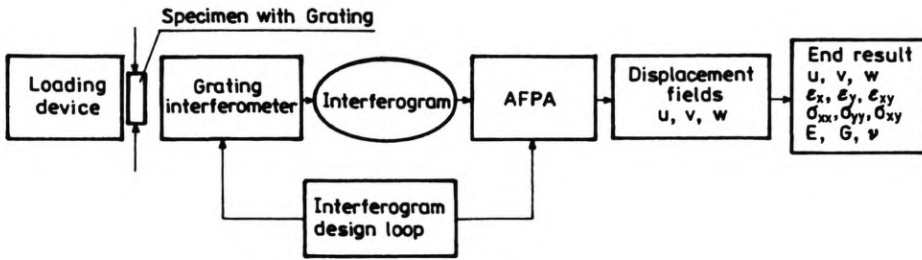
Fig. 1. Scheme of measurement methodology using grating interferometry systems

interferograms is performed alternatively by temporal, spatial or spatial carrier phase shifting methods [11]−[13].

The description of optomechanical arrangement of AGI systems is given in Sec. 2. The phase method of automatic fringe pattern analysis together with the architecture of the software is presented in Sec. 3, and Sec. 4 gives the representative examples of AGI application. As the conclusions, the engineering features of the grating interferometers and areas of their applications are presented in Sec. 5.

2. Grating interferometry systems

2.1. Principle of grating interferometry

The principle of grating interferometry is depicted in Figure 2. A cross-line reflection type diffraction grating of frequency f is produced on the specimen. Two mutually coherent beams, A and B, illuminate the specimen grating obliquely from angles α and $-\alpha$. The specimen grating diffracts the beam A in the $+1$ diffraction order, and the beam B in the -1 diffraction order such that the beams A and
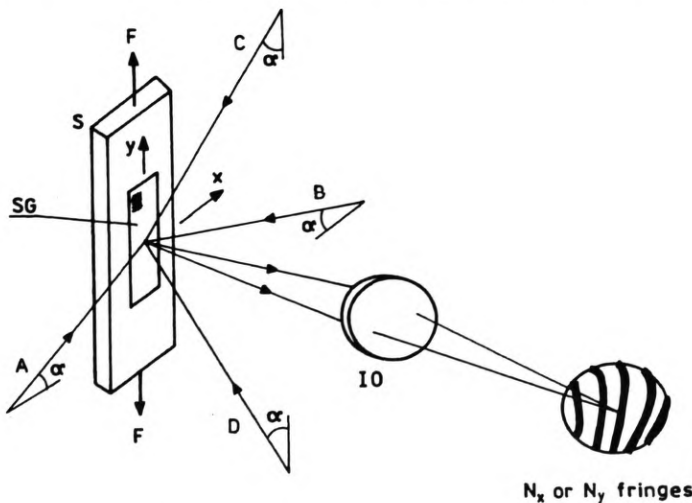

N_x or N_y fringes

Fig. 2. Optical system for grating interferometry. SG − specimen grating, IO − imaging optics

B propagate normally to the specimen grating. When the specimen is subjected to loading, the horizontal and vertical sets of lines are distorted so that the directions of light diffracted in the $+1$ and -1 diffraction orders emerge from the specimen grating with wrapped wavefronts; they coexist in space and generate the interference pattern, namely the contour map of the u displacement field. Similarly, the v displacement field is produced by two beams, C and D. The fringes observed in the interferometer represent a contour map of in-plane displacements with half a period sensitivity and are expressed by

$$I(x,y) = a(x,y) + b(x,y)\cos\left[\left(\frac{4\pi}{d}\right)\begin{matrix}u(x,y)\\ \text{or}\\ v(x,y)\end{matrix}\right].$$ (1)

Numerous different optical schemes [1], [4]−[10] can be arranged to bring the beams A and B, C and D onto the specimen grating.

Here, as discussed in Section 1, three basic types of automatic grating interferometers are presented: the laboratory, workshop and sensor-type systems.

2.2. The laboratory systems (LGI)

Two basic configurations of laboratory systems are considered:

− The three-mirror four-beam grating interferometer (3-MGI) [1], [4], which is specially designed for the specimen grating frequency of 1200 lines/mm and the object size up to 30×30 mm, however, it can work also with the grating frequencies from 900 to 1300 l/mm and a smaller field of view (see Tab. 1). The system may be easily modified for additional out-of-plane displacement w measurement and simultaneous in-plane u and v displacement measurement in one-, two-, or three -channel arrangements.
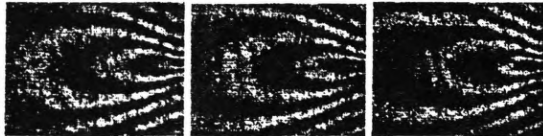
− The one-mirror grating interferometer (1-MGI) with the rotary mounts for specimen and CCD camera [7], which is designed for big components testing (object size up to 100×100 mm), wide range of specimen grating frequencies, from 400 to 1500 l/mm, and odd loading configurations [13].

2.2.1. Three-mirror grating interferometer (3-MGI)

The three-mirror four-beam grating interferometer developed at the Virginia Polytechnic Institute and State University [1], [4] was adopted and modified in author's research group to enable out-of-plane displacement measurement and automatic interferogram anlysis. Figure 3 shows a schematic representation of the basic configuration of one-channel combined 3-MGI/Twyman−Green interferometer, which may be used for sequential u, v and w displacement measurement. To facilitate the automatic computer-aided analysis two approaches implementations of temporal phase shifting technique have been proposed:

− The polarized light approach [14] (Fig. 3 − solid line). The specimen grating is illuminated by two beams with orthogonal polarization and the interference is facilitated by analyser (A). In the case of the u displacement field, opposite directions of polarizations are due to the different number of reflections of two illuminating

T a b l e 1. Fringe pattern design in grating interferometers and the features of automatic fringe pattern analysis methods

Fringe design[*]	FPA method	Type of event	Range[**]	Typical accuracy
$I_i = a + b\cos(\Phi + \delta_i)$	TPS	static	100%	fringe/40
	SPS	dynamic	100% for 3 cameras, 33% for 1 camera	fringe/20
$I = a + b\cos(\Phi + 2\pi f_0 x)$	1-Dir SCPS	dynamic/static	~50%	fringe/20
$I = a + b_1\cos((\Phi_x + 2\pi f_{0_x}) + b_2\cos((\Phi_y + 2\pi f_{0_y})$	2-Dir SCPS	dynamic	~25%	fringe/10

[*] The sinusoidal profile of fringes is assumed.

[**] Range of measurement is understood as the maximum phase gradient which can be analysed by a detector with the same spatial resolution. As TPS is usually performed for a homogeneous interferometric field, this is considered as a reference (100%).
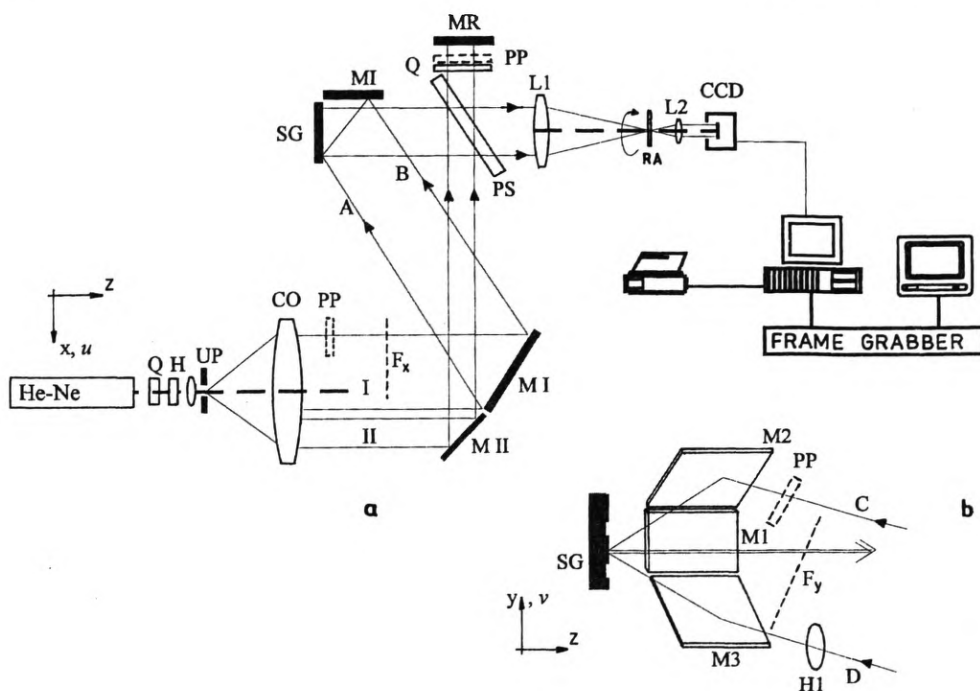
Fig. 3. Optomechanical configuration of the three-mirror four-beam grating interferometer modified for $w(x,y)$ measurements. UP — pinhole system, CO — collimating objective, M1, M2, M3, MR, M I and M II — mirrors, F_x and F_y — slot filters, SG — specimen grating, PS — beam-splitter plate, Q, H, H1 — $\lambda/4$ and $\lambda/2$ phase plates, PP — parallel plate, L1, L2 — imaging optics, RA — rotating analyser

beams (A and B). In the case of measuring the v displacement field, the number of reflections is the same for both (C and D) illuminating beams so the change of polarization in one illuminating beam should be changed by the half-wave plate (H1). Similar situation occurs for the w displacement. In order to supply the orthogonal polarized beams from the Twyman—Green interferometer configuration used for specimen shape measurement, the additional quarter wave-plate is inserted in front of mirror MR. This configuration enables alternative measurement of u, v and w displacements, while the proper parts of beam are cut off and the phase shift is performed by the rotating analyser according to the equation

$$I(x,y) = a(x,y) + b(x,y)\cos[\Phi(x,y) + 2\alpha] \qquad (2)$$

where: $\Phi(x,y) = 4\pi/d[u(x,y)$ or $v(x,y)]$, and α — angle by which analyser was rotated.

 — The tilting parallel plate approach [5], [13] (Fig. 3 — dotted line). In this case, the phase shift is introduced by tilting the plate PP inserted either into the beam C (for v measurements) or into the beam A (for u measurements). The same method is used for automated measurement for the $w(x,y)$ by inserting PP into PS—MR arm of the Twyman—Green interferometer.

The temporal PSM requires stable conditions of measurement, while capturing at least three-phase shifted interferograms. If this requirement is not fulfilled, the GI
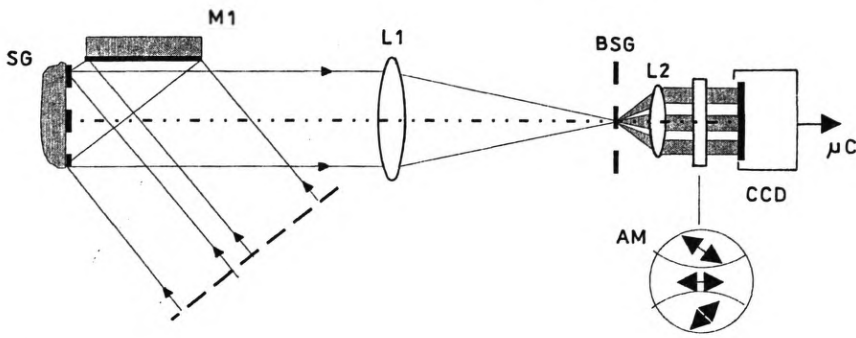
Fig. 4. Triple interferogram polarization grating interferometer. BSG — beam-splitting grating, AM — analyser module, other symbols as in Fig. 3

system should be modified for spatial PSM or spatial carrier PSM. The spatial phase shifting version of GI [14] is shown in Fig. 4. The triple interferogram replication at the output plane is obtained by inserting a sinusoidal transmittance diffraction grating BSG near the focus of objective L1. Spatial separation of the three images is done by proper selection of the BSG frequency. The required phase shifts are introduced by three properly oriented analysers (AM), however, the normalization of intensities of side images with respect to the central one is required.

The spatial-carrier PSM requires introduction of a controlled number of carrier fringes. This is achieved by tilting either the mirror MR (for w displacement) or the mirror M I (for u), or mirrors M2 and M3 (for v). The other option for u and v SCPSM analysis is translating the objective CO in the direction perpendicular to the optical axis of the system. This option also allows us to control compensation for large homogeneous (linear) displacements and to increase the range of measurement.

The one-channel approach (Fig. 3) and SPSM arrangement (Fig. 4) restrict applications of the system to static events when sequential measurements of u, v and w displacements are sufficient. However, the 3-MGI may be modified for two- and three-channel arrangements in which the methods described previously are applied to produce simultaneously u, v and w displacement interferograms [15] designed for one- and two-directional method of spatial carrier PSM [16].

Figure 5 presents two-channel system which may provide alternatively the simultaneous two interferograms of u and v displacements (solid line) or one interferogram of w displacement and combined cross-line fringe pattern for u and v (solid + dashed lines). In the system shown in Fig. 5 by solid lines, the polarization method is used to separate the u and v displacement patterns [15]. Grating G (frequency of 120 lines/mm) is applied as an additional beam-splitter, and the analyser A is used to select orthogonally polarized diffracted orders of the specimen grating (SG), which form the u and v fringe patterns. These separated interferograms are captured simultaneously by CCD camera and analysed by SCPS method. For measuring the out-of-plane displacements w, the Twyman—
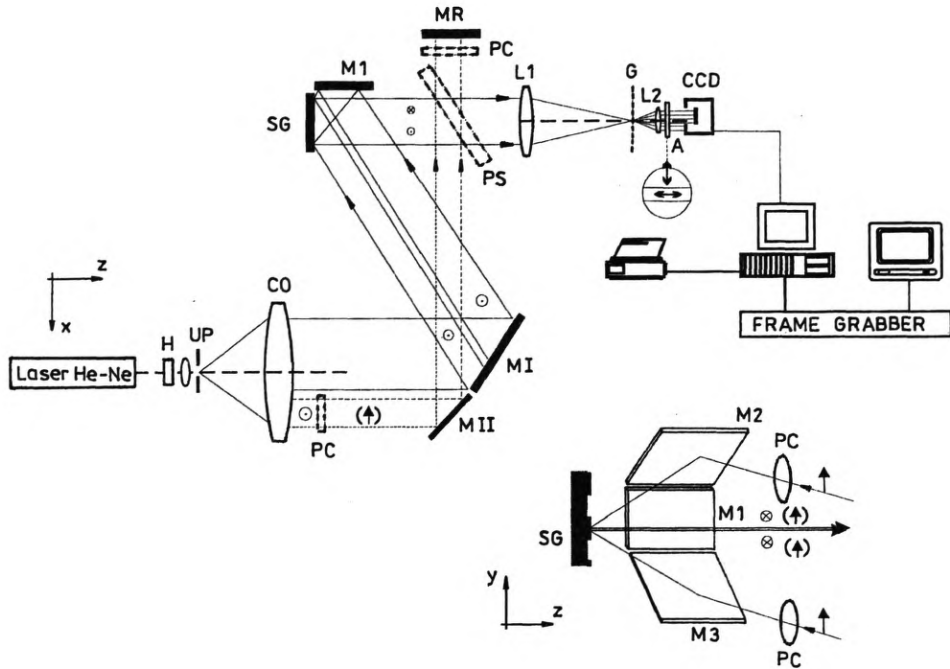
Fig. 5. Two-channel grating interferometer for simultaneous measurement of u and v displacements and, after modifications (dashed lines), for u, v and w displacements analysis. UP — pinhole system, CO — collimating objective, M1, M2, M3, M I, M II — mirrors, PC — compensators, L1, L2 — imaging optics, SG — specimen grating, G — beam-splitter grating, A — analyser, PS — beam-splitter plate

Green interferometer configuration is adopted [5]. It uses a part of the illuminating beam behind the collimating system UP — CO. Now, for a simultaneous analysis of all displacement patterns, the state of polarization for u and v patterns forming beams must be linear in the vertical direction. The beams creating the w displacement pattern have perpendicular polarization. This requirement can be realized by using compensators PC. In this way, the two-pattern, sum-type u and v interferogram is created in one channel, and the interferogram of w is obtained in the second channel. The two-directional spatial carrier phase-shifting method is used for analysis of the two-pattern interferogram in order to retrieve both u and v displacement components.

For practical use, the three-channel system for simultaneous automatic capturing and analysis of u, v and w displacements [15] is presented in Fig. 6. It comprises two polarization separated channels for u and v displacement field determination. The third channel for w displacement measurement is separated by using the illumination beam of different wavelength and interference filter (IF). Two semiconductor lasers are used, LD1 with $\lambda_1 = 650$ nm and LD2 with $\lambda_2 = 670$ nm. The interferograms are stored by three synchronized CCD cameras and are analysed by SCPS method.
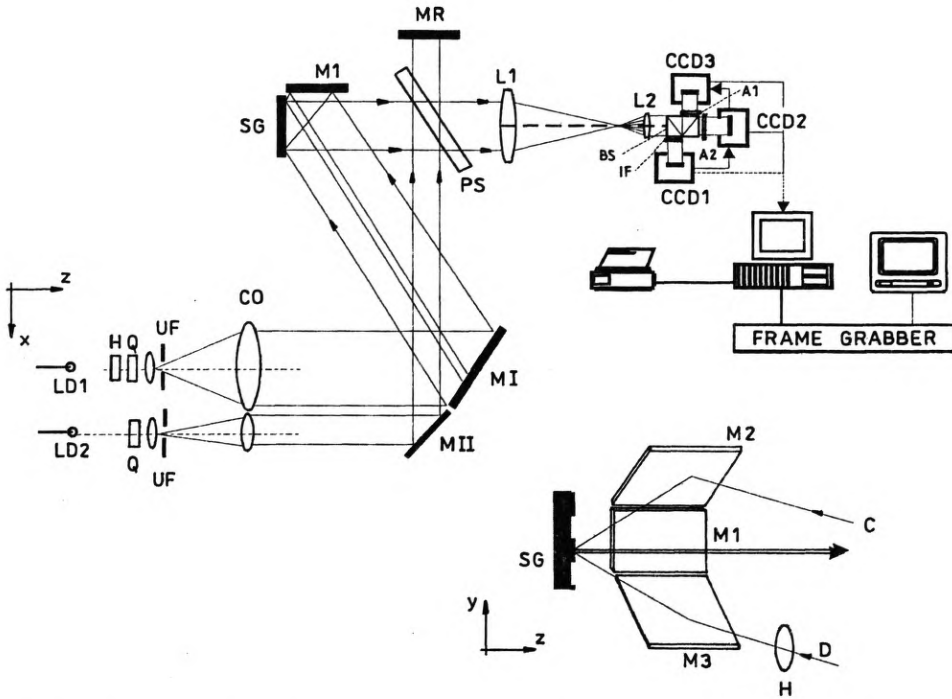
Fig. 6. Three-channel interferometer system for simultaneous automatic analysis of u, v and w displacements. LD1, LD2 — semiconductor lasers ($\lambda_1 = 650$ nm, $\lambda_2 = 670$ nm), H — $\lambda/2$ plate, Q — $\lambda/4$ plate, BS — beam-splitter, A1, A2 — analysers, IF — interference filters (for other symbols see Fig. 5)

The numerous versions of 3-MGI prove the flexibility of the arrangement for various measurement and interferograms design requirements. However, if a measurement of a big component is required, large dimension of the mirrors of interferometer head and collimator lens would make the cost of the system prohibitively high. Also the mirror configuration design is well fitted for the specimen grating frequency of 1200 lines/mm, while the measurement area decreases rapidly with the change of frequency applied (see Tab. 2, p. 230). These are the reasons why another grating interferometry configuration is sometimes recommended in laboratory works.

2.2.2. One-mirror grating interferometer (1-MGI)

The one-mirror grating interferometry arrangement 1-MGI enables us to use the specimen gratings with various frequencies [17] and to perform tests on big elements (up to 100×100 mm) [7] as well as provides a convenient way of applying and measuring load in odd configurations. Two coherent beams illuminate symmetrically the diffraction grating fixed to the sample, as shown in Fig. 7. One mirror head and the rotary mounts of the specimen and CCD camera enable the sequential measurement of u and v displacements. Phase shifting is introduced by tilting the parallel plate PP or by polarization method.
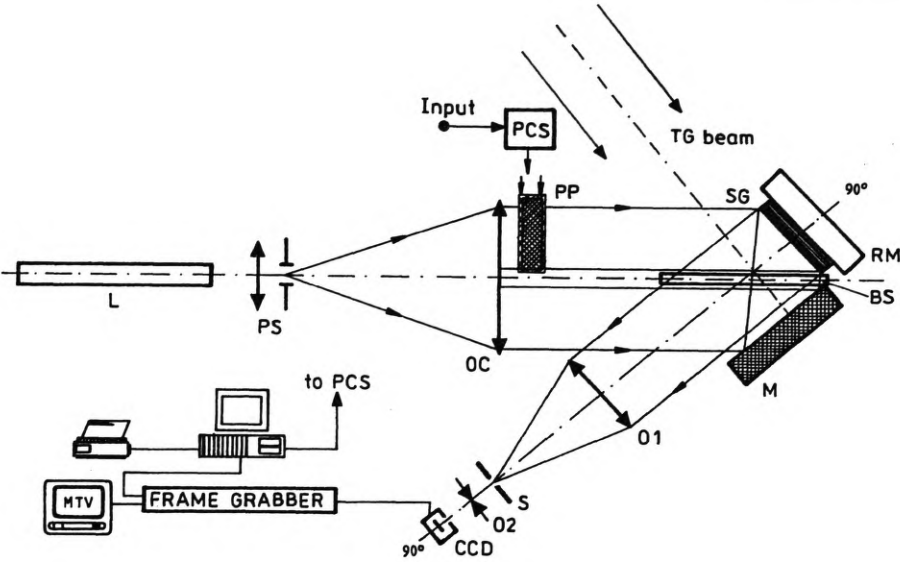
Fig. 7. Scheme of the one-mirror grating interferometry system, L — He-Ne laser, PS — pinhole system, OC — collimator objective, PCS — phase shift controller, PP — parallel plate, O1, O2 — imaging objectives, SG — sample with diffraction grating, RM — rotary mirror, M — mirror, BS — beam-splitter, TG beam — collimated beam to Twymann—Green interferometer

The system may be modified for *w* displacement measurement by introducing the second collimated beam and inserting an additional beam-splitter (BS). In this way, the specimen grating (SG), mirror (M) and beam-splitter form a Twyman—Green interferometer, as shown in Fig. 7. The system is very easy to arrange with typical optomechanical elements and can be adapted to various sensitivities and ranges of measurements required (Tab. 1), however, it may be applied to static measurements only. A good example of 1-MGI's application is residual stress analysis [7].

2.3. Workshop, portable system

The workshop, portable system enables analysis of transient events, displacements and strain measurements directly on a standard loading machine (Instron, Schenck) and/or unstable (often industrial) environment [18]. The optomechanical arrangement, shown in Fig. 8, is based on achromatic grating interferometer (AGI) scheme [1], [8] modified for the automated analysis of interferograms captured by CCD camera. Additionally, a video recorder for storing sequential fringe patterns during dynamic loading may be applied. It was proved that due to applying the compensating grating (CG), the system is relatively insensitive to vibrations and can be used directly on a loading machine. The full configuration of AGI, using cross-type specimen grating (SG), for in-plane displacement measurement in two mutually perpendicular directions (*x* and *y*) is shown in Fig. 9. Two collimated beams I and II illuminate two compensator gratings, CGX and CGY. The grating CGX, mirrors M1X and M2X work in horizontal plane for *u* displacement measurement.
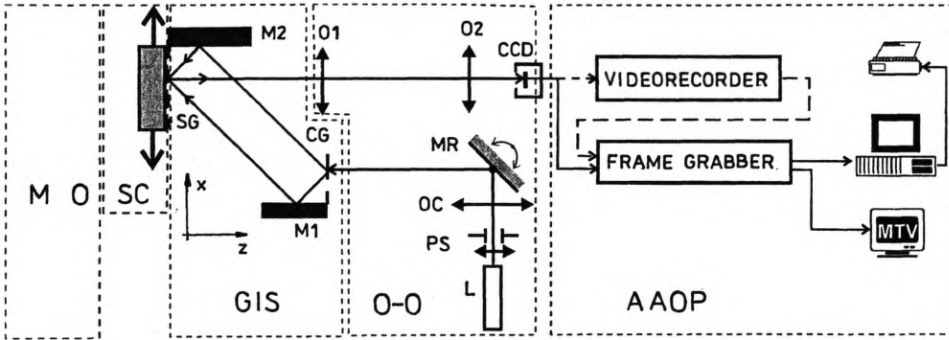
Fig. 8. Scheme of portable, automatic grating interferometry system. L — He-Ne laser, PS — pinhole system, CO — collimating objective, MR — mirror, CG — compensator grating, SG — specimen grating, M1 and M2 — interferometer mirrors, O1 and O2 — imaging lenses, MO — loading machine, SC — sample, GIS — grating interferometer head, O—O — illumination/detection module
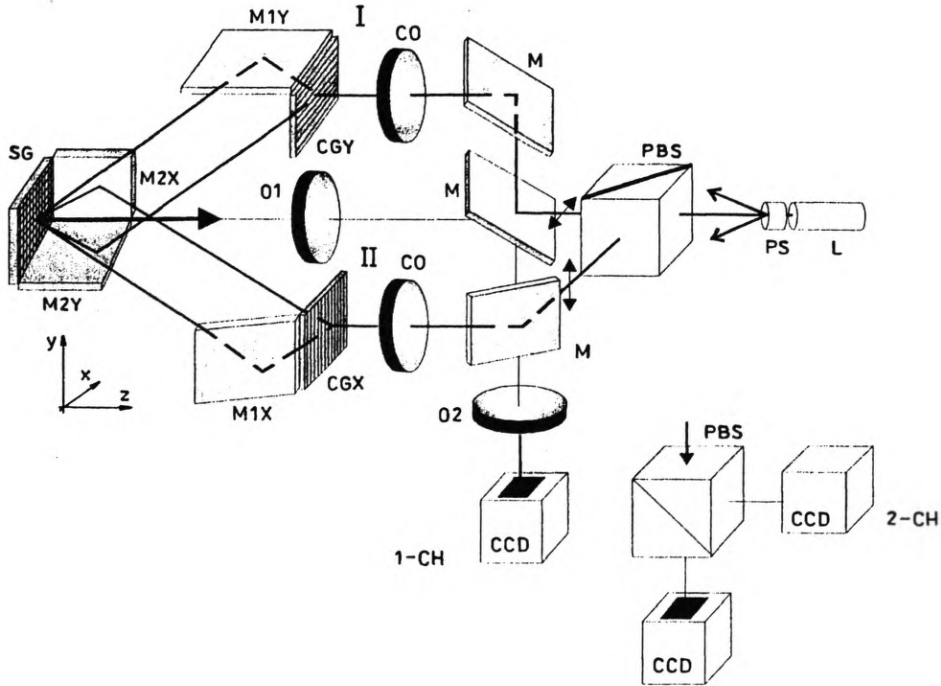

Fig. 9. Scheme of achromatic grating interferometer for *u* and *v* displacement measurements. 1-CH — one- and 2-CH — two-channel versions, SG — cross-type specimen grating, CGX and CGY — compensator gratings, M1X, M1Y, M2X and M2Y — interferometer mirrors, PBS — polarization beam-splitter, I and II — illuminating beams

Analogous system (grating CGY, mirrors M1Y and M2Y) working in vertical plane are used for *v* displacement measurement. The system may work in one-channel (1-CH, Fig. 9) and two-channel configurations (2-CH). In 1-CH option, the analysis

may be performed alternatively for u and v displacements by SCPSM, or for two–directional SCPSM for simultaneous analysis of both displacements [13], [16]. In the latter case, the sum-type cross-interferogram is obtained, while two orthogonally polarized pairs of beams interact. In 2-CH option, the single interferograms for u and v displacements are obtained simultaneously at two CCD cameras due to inserting the second polarization beam-splitter at the output of the system. This second option allows us to enlarge the measurement range and accuracy of simultaneous u and v analysis, when compared with two-directional SCPSM.

2.4. Fibre optics grating interferometer sensor (FOS)

The implementation of bulk optics version of grating interferometers is often restricted due to the relatively large size of the system. The fibre optics version of GI allows a reduction in the number of optical components to be adjusted. Due to mechanical flexibility of fibres and the small size of fibre optics components, miniaturization of the sensor can be achieved. An initial version of such a sensor is shown in Fig. 10 [10]. A single mode laser diode (*e.g.*, Sharp LT024 emitting at 780 nm) is coupled with single mode optical fibre via a Faraday isolator and
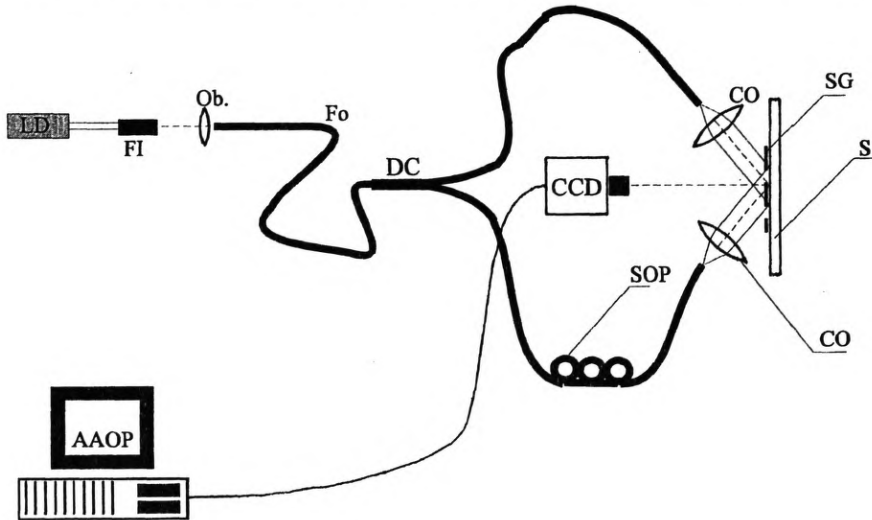

Fig. 10. Experimental arrangement of fibre optic grating interferometer. LD — laser diode, FI — Faraday isolator, Ob — microscopic objective, Fo — single mode fibre, CO — collimating objective, SOP — fibre optic state of polarization controller, S — specimen, SG — specimen grating, DC — directional coupler 50:50

microscope objective. The light is divided into two illuminating beams by 50:50 directional coupler. The fibre optic state of polarization (SOP) controller allows matching SOP of the interfering beams. In principle, the sensor may produce the interferogram designed for temporal phase shifting, while using piezoelectric modulator [19] or laser diode wavelength modulation [20]. However, it should be rather designed for rapid, easy measurement in unstable environment, so the spatial carrier

phase shifting method is preferred. The initial mechanical configuration of both illuminating beams should assure the proper carrier frequency for the chosen CCD sampling resolution. The sensor is designed for the a priori chosen: specimen grating frequency (usually one-directional), illumination beam wavelength, small measurement area (up to 2×2 mm). Therefore it does not allow flexibility of the tests performed, however, FOS may become a compact, convenient tool for on-structure and field in-plane displacement/strain measurements.

3. Automatic analysis of the results

The interferograms obtained in grating interferometers have to be analysed automatically by one of the phase fringe pattern analysis methods. The optomechanical GI systems allows to design interferogram according to the requirements of temporal (TPSM), spatial (SPSM) and spatial-carrier (SCPSM) (one- and two-directional versions) of phase shifting methods (see Tab. 1). The general architecture of automatic fringe pattern analysis (AFPA) system is shown in Fig. 11.
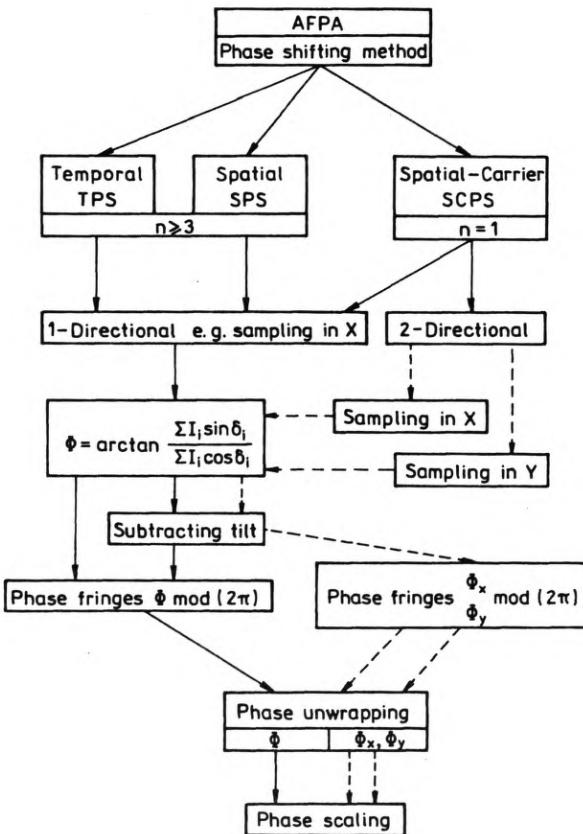

Fig. 11. Architecture of automatic fringe analysis (AFPA) system (n — number of fringe patterns)

The high accuracy TPSM based on five intensity algorithm is used in GI systems for measurements of static events in vibration-free environment. Investigation of dynamic processes and measurement in unstable environment require an analysis on the base of a single interferogram. Additionally, the problem of simultaneous analysis of the information about two events (u and v displacement fields) coded into a cross-interferogram should be solved.

These problems have to be approached by one of the spatial techniques of fringe pattern analysis [12], including 2-D Fourier transform or spatial carrier phase-shifting methods. SCPS method combines the simplicity of calculations given by phase-shifting technique and the advantages of single interferogram analysis provided by Fourier transform method. That was the reason why SCPS in its one- and two-directional versions [13] was implemented in laboratory, portable and sensor-type grating interferometry systems.

The main requirement for SCPS method is introducing the proper carrier frequency f_0 so that the fringe pattern equation is modified

$$I(x,y) = a(x,y) + b(x,y)\cos[\Phi(x,y) + 2\pi f_0 x] \qquad (3)$$

where the most frequently used carrier frequency f_0 is four times lower than the sampling frequency of the detector in x-direction. In this case, the phase-shifting technique is applied to the intensities captured in the sequential pixels. If the following assumptions are fulfilled:

— the carrier frequency such that the phase in the sequential pixels differs by $\pi/2$,

— slowly varying phase $\Phi(x,y)$, background $a(x,y)$ and contrast $b(x,y)$ functions, the phase is calculated using the 5-frame, error compensating algorithm proposed in [21]

$$\Phi(i,j) = \arctan \frac{-I(i-2,j) + 4I(i-1,j) - 4I(i+1,j) + I(i+2,j)}{I(i-2,j) + 2I(i-1,j) - 6I(i,j) + 2I(i+1,j) + I(x+2,j)} \qquad (4)$$

where (i,j) is the discrete version of spatial coordinate (x, y) expressed in the number of sampling point. The continuous phase function is obtained by applying unwrapping procedure to the Φ mode (2π) given above. If the simultaneous analysis of two displacement maps is required, the cross-pattern sum-type interferogram with the properly introduced carrier frequencies in x and y directions has to be considered

$$I(x,y) = a(x,y) + b_1(x,y)\cos[\Phi_x(x,y) + 2\pi f_{0x}x] + b_2(x,y)\cos[\Phi_y(x,y) + 2\pi f_{0y}y] \quad (5)$$

where: $\Phi_x(x,y) = \dfrac{4\pi}{d}u(x,y)$, $\Phi_y(x,y) = \dfrac{4\pi}{d}v(x,y)$ and the carrier frequencies fulfil the conditions: $f_{0x} = M/4$, $f_{0y} = N/4$, with M and N being the sampling frequencies of the detector in x and y directions.

In order to retrieve both component functions, the cross-pattern interferogram has to be sampled separately in x and y directions. The phase retrieving SCPS process is sensitive to reference grid, so the phases coded in both component patterns
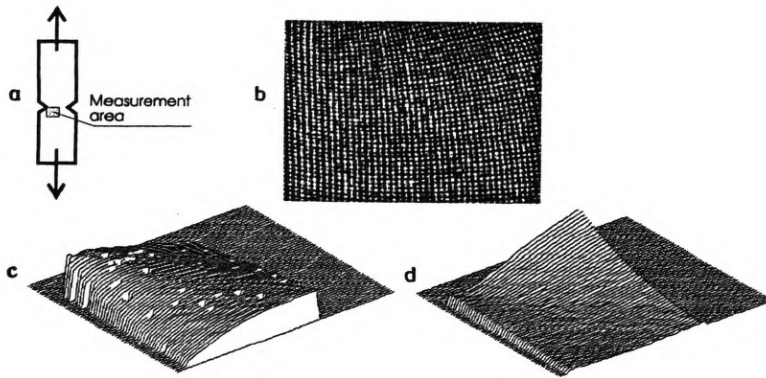
Fig. 12. 2-directional SCPS analysis for simultaneous *u* and *v* displacement measurements in tensile steel beam with crack: **a** — sample configuration, **b** — cross-pattern sum-type interferogram, **c** — 3-D plot of *u* displacement, **d** — 3-D plot of *v* displacement

can be obtained separately, using the same algorithm as that described above. An example of 2-directional SCPS analysis of *u* and *v* displacement fields obtained simultaneously is shown in Fig. 12.

The basic output information obtained after automatic fringe pattern analysis are the displacement fields *u*, *v* and *w*. The software of AFPA includes also the procedures for strains ε_x, ε_y, ε_{xy} and calculation of engineering constants, such as Young's moduli, Poisson's ratios or shear moduli.

The SCPS analysis can be applied to the interferograms captured and digitized directly during the experiment as well as stored on the video recorder tape. The interferograms recorded during the transient event (crack propagation, relaxation process, *etc.*) can be viewed and the selected frames are transferred to computer for quantitative analysis. In order to prevent the degradation of the image quality, the SVHS recording system is strongly adviced (see the error analysis in [9]). The fringe pattern design capabilities of various grating interferometers in connection with their applications are summarized in the conclusions of the paper (Fig. 17).

4. Examples of recent application

The systems presented are used to wide range of static and dynamic analysis in experimental mechanics and material science problems. Below, some recent examples are presented with the special emphasis put on the analysis of transient problems.

4.1. Application of the laboratory system (LGI)

Monitoring and analysis of the bahaviour of new technological materials, *e.g.*, composite materials or determination of local material constants in elastic-plastic problems (fracture mechanics, micromechanics, contact problems) are the modern tasks of grating interferometers. As an example, the analysis (performed on 3-MGI) of the cracking process in a carbon/epoxy UD sample with two ply drop-offs [6]
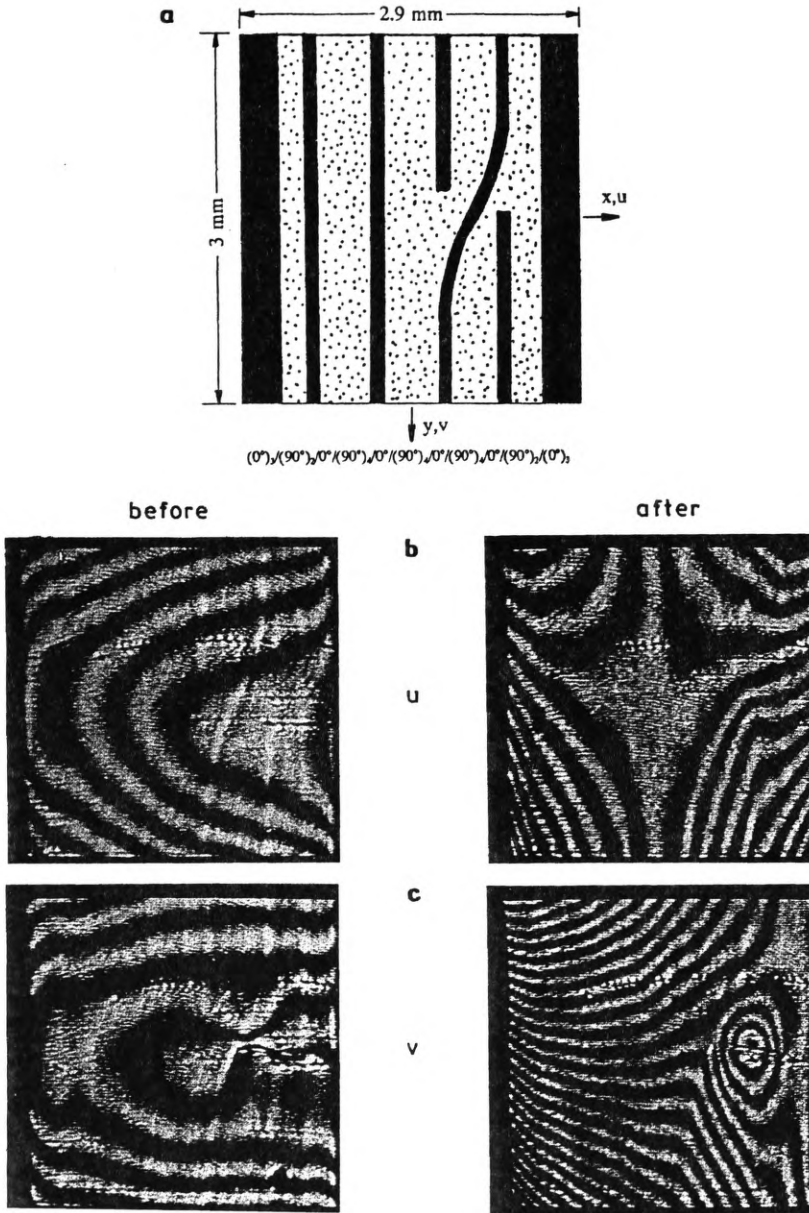
Fig. 13a—c (Fig. 13d—f, see the next page)

is shown in Fig. 13. The specimen (Fig. 13a) was loaded in four-point bending rig and the grating was attached to the middle region, where it is under pure bending. The u and v displacement fields were monitored simultaneously and were captured before and after a crack had been formed at the ply drop-off at the same bending moment. The u and v displacement maps were obtained (Fig. 13b,c) and were used for ε_x, ε_y
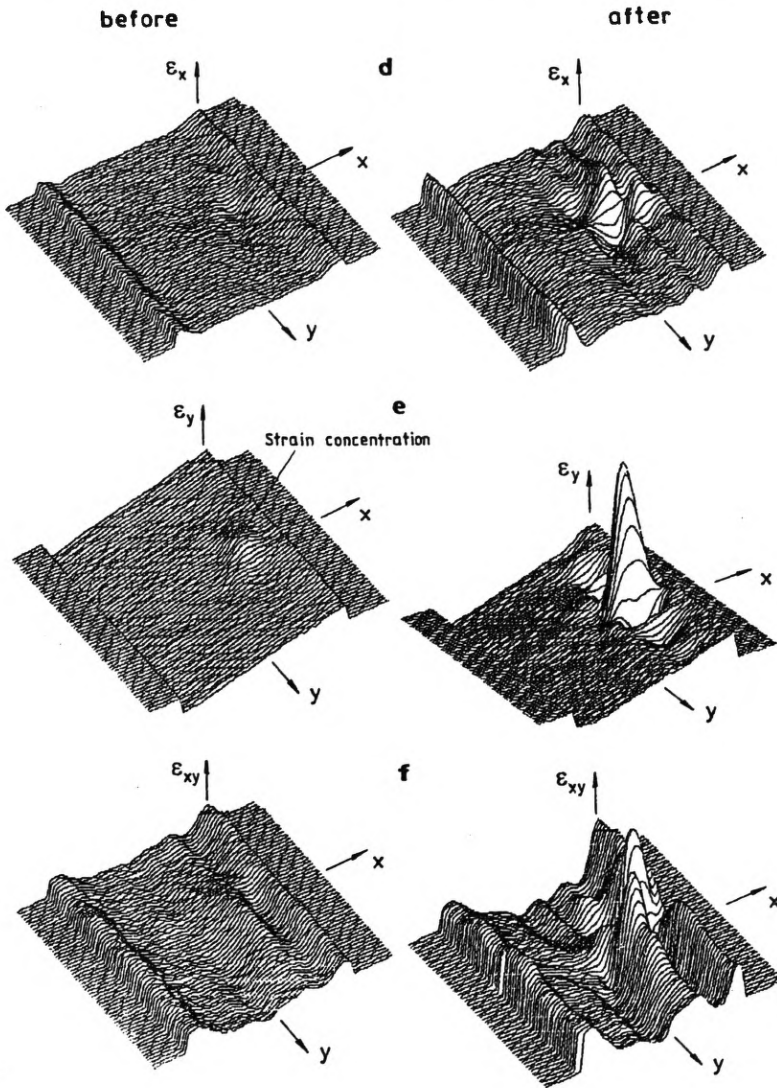
Fig. 13. Analysis of the cracking process in a carbon/epoxy sample with two ply drop-offs: a — laminate lay-up geometry of the specimen, interferograms indicating b — u and c — v displacement fields before and after the crack and the resultant strain maps d — ε_x, e — ε_y and f — ε_{xy} also before and after crack

and ε_{xy} strain calculations (Fig. 13d−f). During loading the strain concentration arised as indicated in Fig. 13e at the ply drop-off. After the crack was formed, the load released by crack was transferred to neighbouring regions and redistribution of the state of strain occurred which resulted in strain concentrations of ε_x, ε_y, ε_{xy} around the crack.

The analysis of residual strains distribution in a cross-section of a railway rail is given as an example of application of 1-mirror laboratory system. Due to big size and odd shape of samples (70 × 50 mm) the system with rotary mounts of the
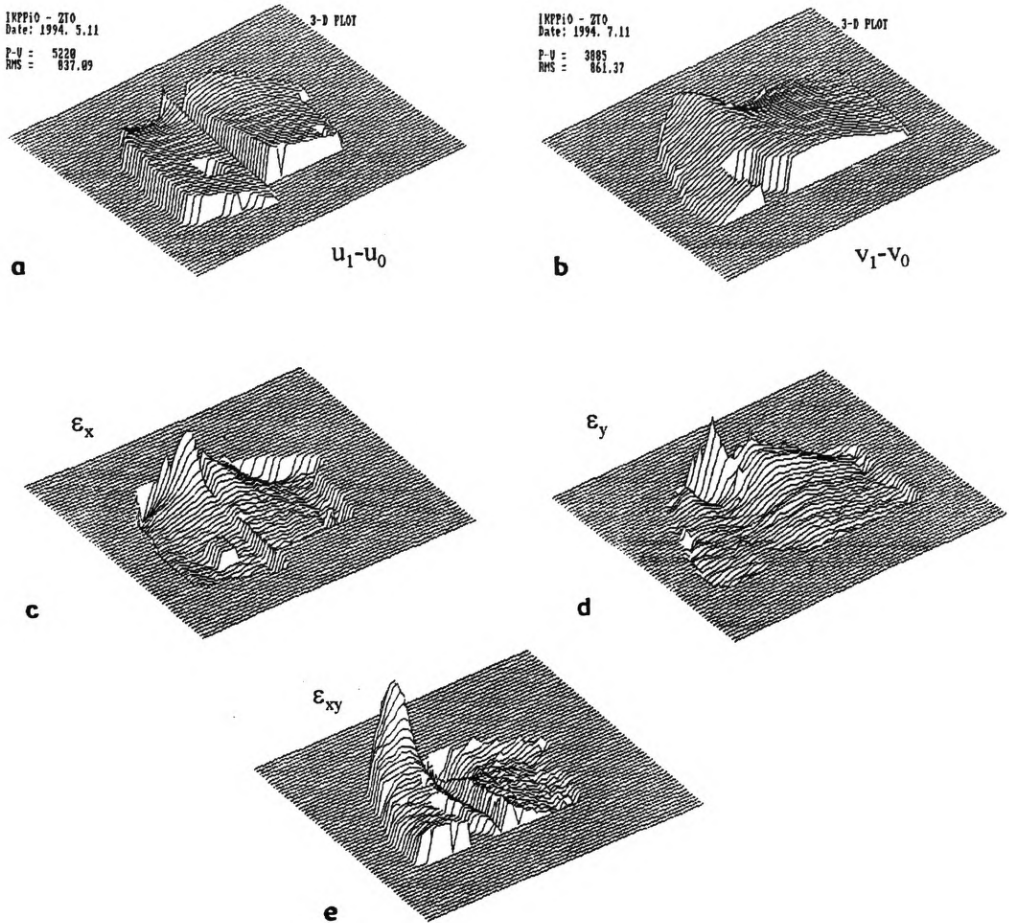
Fig. 14. 3-d plots of the calibrated displacement fields in railroad rails after thermal stress relieving process: a — $(u_1 - u_0)$, b — $(v_1 - v_0)$, and the strain maps c — ε_x, d — ε_y, e — ε_{xy}

specimen and CCD camera was necessary [7]. The u and v fringe patterns were collected before (u_0, v_0) and after (u_1, v_1) the stress releasing by thermal method. The difference displace-ments $(u_1 - u_0)$ and $(v_1 - v_0)$ were used for ε_x, ε_y and ε_{xy} calculations in transverse and oblique rail slices (Fig. 14). The methodology described above [7] was chosen as the experimental basis for the hybrid analysis of 3-D residual stress state in railroad rails [22].

4.2. Application of the workshop system (WGI)

The workshop grating interferometry system was applied to wide range of fracture mechanics problems. Figure 12 shows an application of two-directional SCPS method to simultaneous u and v displacement analyses in a tensile steel beam specimen with a notch under tensile load. For monitoring and analysis of in-plane displacement fields during fatigue loading of titanium alloy beam with a notch in
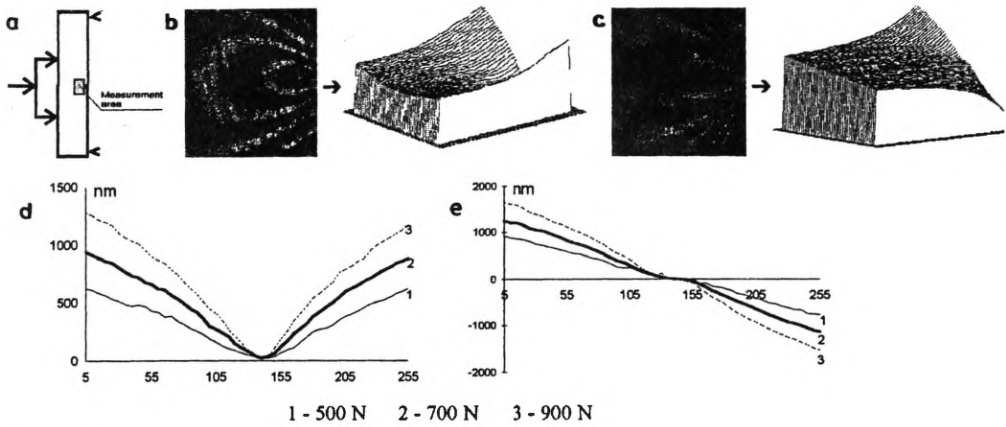
Fig. 15. Measurement results obtained in WGI with video recorder during monitoring of displacement fields in titanium alloy beam: **a** — loading configuration, **b** — u and **c** — v displacement fields under the load $F = 900$ N, **d** — u and **e** — v displacement cross-sections obtained for different load at the crack tip in the direction perpendicular to the crack
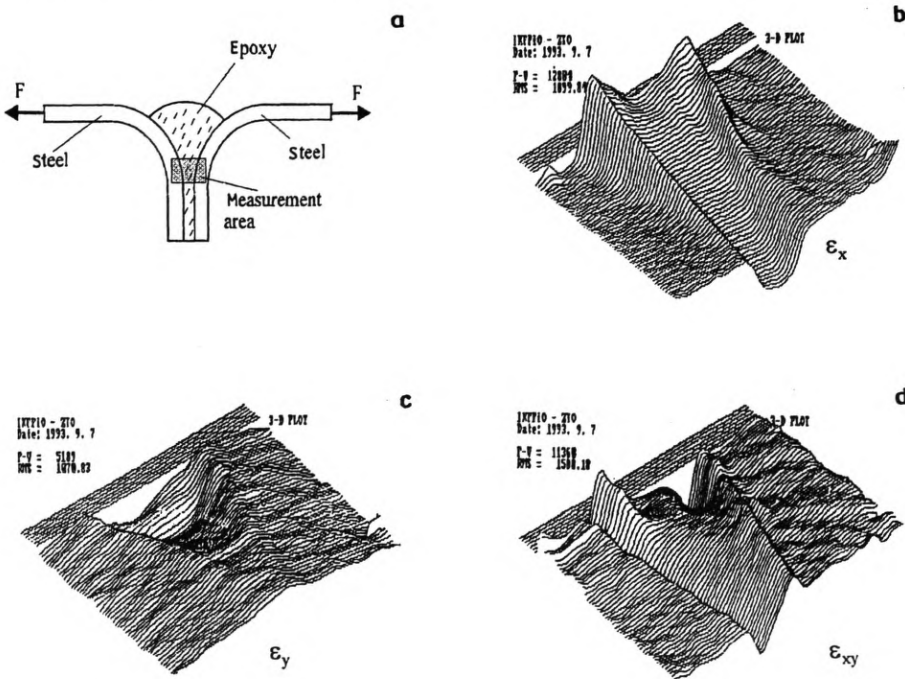

Fig. 16. Displacement and strain measurements in the adhesive steel/epoxy/steel joint: **a** — specimen geometry and loading configuration and 3-D plots of strain fields, **b** — ε_x, **c** — ε_y, and **d** — ε_{xy}, respectively

four point bending configuration (Fig. 15a), the interferograms were recorded by video recorder [9]. The specimen was subjected to cyclic load in the range from 0 to 3 kN and the frequency of 5 kHz. After 2000 cycles the grating was transferred on the specimen and the displacement fields for next cycle were monitored. The exemplary

T a b l e 2. Engineering features of the grating interferometers

Features AGI*	Grating frequency [l/mm]	Measuring area [mm]	Sensitivity per fringe [nm]	Accuracy (part of fringe)	Range of displace-ment*** [μm]	Sensitivity to vibrations	Method of analysis	Modifications for	
								w	multichannel
3-MGI	900÷1200 +1300	2×2÷30 ×30÷2×2	556÷385	±1/40	60÷40	high	TPS, SPS SCPS	+	+
1-MGI	400÷1500	up to 100×100**	1250÷333	±1/40	120÷30	high	TPS, SPS SCPS	+	−
WGI	1200	up to 25×25	417	±1/20	40	low	SPS, SCPS	−	+
FOS	single working frequency from the range 400÷1500	recommended 2×2	1250÷333	±1/10	120÷30	low	SCPS	−	−

* The systems are considered to work in air (no immersion).
** Depending on the illuminating beam diameter.
*** The range of displacement determined for the detector with 512×512 resolution.

3-D plots of u and v displacements for the load $F = 900$ N are shown in Figs. 15b,c. The cross-sections of these fields obtained for different loads ($F = 500, 700, 900$ N) at the crack tip in the direction perpendicular to the crack are given in Figs. 15d and e.

Another application presented refers to the problem of testing of displacement/strain fields in adhesive joints and analysis of stress relaxation in such components. Figure 16 shows the steel/epoxy/steel joint subjected to the tensile load and the distributions of strains ε_x, ε_y and ε_{xy} calculated by differentiation of the u and v displacement fields obtained in WGI.

5. Conclusions and recommendations

The excellent characteristics of grating interferometry as an optical method of testing and recent achievements in design and technology of optomechanical and image acquisition and processing devices enable us to propose the whole range of experimental convenient systems for recent applications of experimental mechanics, material engineering and industrial control. Table 2 summarizes the features of systems presented in the paper.
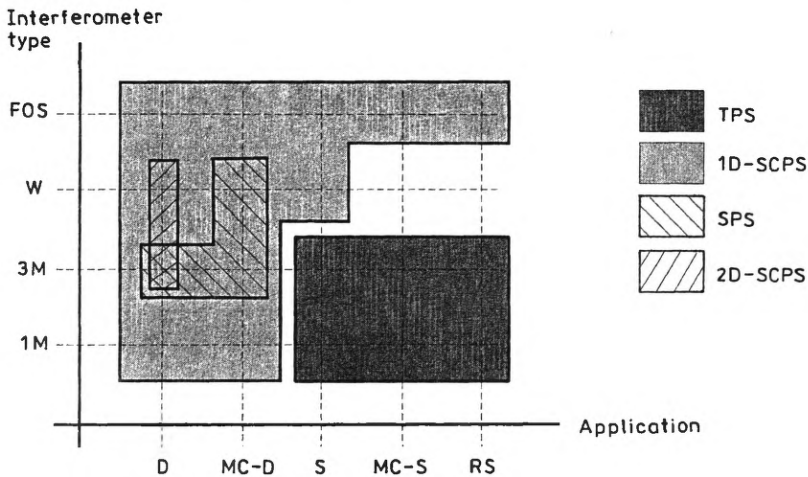

Fig. 17. General areas of applications of various types of grating interferometers *vs* the recommended fringe pattern analysis. Applications: D — dynamic, MC-D — material constants/dynamic, S — static, MC-S — material constant/static, R — residual stresses. Interferometers: 1-MGI, 3-MGI, WGI and FOSGI

The variety of optomechanical solutions fulfils recent instrumentational requirements, including adaptive fringe pattern design, macro/microscale measurement ability, analysis of transient phenomena and measurements in unstable environment. The general areas of applications of laboratory, workshop and fibre optic version of grating interferometry versus the recommended fringe pattern analysis are shown in Fig. 17.

The most recent examples of GI applications as an experimental tool in hybrid methods of stress analysis include: fracture mechanics, residual stresses, relaxation processes, measurement of local material constants, heat transfer in electronic packaging, contact problems, modelling local phenomena in structural joints, surface layers, composite materials, material grains interaction and many others.

The automated grating interferometry provides reliable data for the feedback process combining mathematical and physical models of real structure and material behaviour.

References

[1] POST D., HAN B., IFJU P., *High Sensitivity Moiré — Experimental Analysis for Mechanics and Materials*, Springer-Verlag, 1994.

[2] LAERMAN K. H., *New Perspectives for Laser Metrology — Vision and Instruction*, [In] *Physical Research*, Vol. 19, [Eds.] W. Jüptner, W. Osten, Akademie Verlag, 1993, pp. 15–23.

[3] KUJAWIŃSKA M., *Optical Methods for Hybrid Analysis of Structure*, SPIE Short Course Materials at SPIE Annual Meeting, San Diego 1993.

[4] CZARNEK R., Opt. Laser Eng. **15** (1991), 93.

[5] KUJAWIŃSKA M., SALBUT L., CZARNOCKI P., Proc. SPIE **2004** (1993), 282.

[6] POON C. Y., KUJAWIŃSKA M., RUIZ C., J. Strain Analysis **28** (1993), 79.

[7] KUJAWIŃSKA M., SALBUT L., Proc. SPIE **2324** (1994), 248.

[8] CZARNEK R., Opt. Laser Eng. **13** (1990), 93.

[9] SALBUT L., KUJAWIŃSKA M., DYMNY G., Proc. SPIE **2342** (1994), 58.

[10] KOZŁOWSKA A., Proc. SPIE **2341** (1994), 124.

[11] KUJAWIŃSKA M., Opt. Laser Eng. **19** (1993), 261.

[12] KUJAWIŃSKA M., *Spatial Phase Measurement Methods*, [In] *Interferogram Analysis: Digital Fringe Measurement Techniques*, [Eds.] D. W. Robinson, G. Reid, IOP Publ., Bristol, Philadelphia 1993, pp. 141.

[13] PRYPUTNIEWICZ R. J., KUJAWIŃSKA M., *FEM/moiré interferometry hybrid analysis of stress relaxation in a microconnector*, Proc. INTERPACK'95, ASME, New York 1995, pp. 1179.

[14] SALBUT L., PATORSKI K., KUJAWIŃSKA M., Opt. Eng. **31** (1992), 434.

[15] SALBUT L., *Multichannel system for automatic analysis of u, v and w displacements in grating interferometry*, [In] *Physical Research*, Vol. 19, [Eds.] W. Jüptner, W. Osten, AAkademie Verlag, 1993, pp. 282.

[16] KUJAWIŃSKA M., PIRGA M., *Fringe pattern analysis for the investigation of dynamic processes in experimental mechanics*, [In] Physical Research, Vol. 19, [Eds.] W. Jüptner, W. Osten, Akademie Verlag, 1993, pp. 391.

[17] KUJAWIŃSKA M., TKACZYK T., PRYPUTNIEWICZ R., Proc. SPIE **2544** (1995), in press.

[18] HAN B., GUO Y., LIM C. K., *Application of interferometric techniques to verification of numerical model for microelectronics packaging design*, Proc. INTERPACK'95, ASME, New York 1995, pp. 1187–1194.

[19] JOENATHAN C., KHORANA B. M., Opt. Eng. **2** (1992), 315.

[20] TATAM R. P., DAVIES J. C., BUCKBERRY C. H., JONES J. D. C., Opt. Laser Technol. **22** (1990), 317.

[21] SCHMIT J., CREATH K., *Extended averaging technique for deviation of error-compensating algorithms in phase-shifting interferometry*, submitted to Applied Optics, 1995.

[22] MAGIERA J., ORKISZ J., Proc. SPIE **2342** (1994), 314.